

Electrostatic Precipitator Operation at Corona Quenching Conditions – Theory, Simulation and Experiments

Christian LUEBBERT
Brandenburg Techn. Univ.
Cottbus
Germany
Luebbert@mvt.tu-cottbus.de

Ulrich RIEBEL
Brandenburg Techn. Univ.
Cottbus
Germany
riebel@mvt.tu-cottbus.de

1 Summary / Abstract:

Mathematical models of different complexity are developed for the description of the residence time dependent current uptake in a tube wire type electrostatic precipitator under conditions of corona-quenching. For a simple tube-wire geometry, corona quenching by concentrated aerosols is studied theoretically, by numerical simulation and experiments.

The numerical simulations are executed in 1D, whereby various levels of complexity (including particle and ion space charge, ion extinction, lateral mixing (turbulent diffusion), particle charge and size distribution, charging and agglomeration kinetics) are attained.

Simulation predictions of the current uptake behaviour are compared to experimental results from batch type and continuously operated electrostatic precipitators.

2 Introduction

Corona quenching occurs when highly concentrated aerosols enter into an electrostatic precipitator. The current uptake drops dramatically and at the same time, the emission of particles goes up and sparking occurs. Usually, corona quenching is seen as a disturbance of regular electrostatic precipitator operation. Here we discuss corona quenching as a special (and very efficient) regime of ESP operation, which however requires special rules of design and operation.

2.1 The electric field in an ESP under consideration of particle attached space charge

The knowledge of the local electric field in an ESP is fundamental for calculating particle charging kinetics and particle migration velocity. In common one stage ESPs, the electric field is, at least beyond a certain distance from the corona electrodes, mainly governed by the space charge in the ESP. For the axisymmetric case of a tube wire type ESP, the distribution of the electric field can be calculated, when a constant particle attached space charge is assumed over the ESP's cross-section.

Assuming additionally a constant mobility of the ions while travelling from the corona wire to

the collecting electrode and the applicability of the continuity equation for the ionic current (the loss of ions due to particle charging is discussed later) one finds the local ion concentration to depend on the radius coordinate as follows:

$$\rho_i(r) = - \frac{\rho_{ip}}{1 + LambertW_{-1} \left[\frac{\left(\frac{2\pi r_w LZ_i \rho_{ip}}{I} \right) E_{onset} + 1}{\exp \left\{ \left(\frac{2\pi r_w LZ_i \rho_{ip}}{I} \right) \left(E_{onset} + \frac{\rho_{ip} (r^2 - r_w^2)}{r_w 2\epsilon_0} \right) + 1 \right\}} \right]}$$

(Eq. 1)

Here, the use of the <-1-branch of the LambertW-function is indicated by the index -1.

The corresponding electric field distribution is found to be:

$$E(r) = - \frac{I}{2\pi r_w LZ_i \rho_{ip}} \left[1 + LambertW_{-1} \left[\frac{- \left(\frac{2\pi r_w LZ_i \rho_{ip}}{I} \right) E_{onset} - 1}{\exp \left\{ \left(\frac{2\pi r_w LZ_i \rho_{ip}}{I} \right) \left(E_{onset} + \frac{\rho_{ip} (r^2 - r_w^2)}{r_w 2\epsilon_0} \right) + 1 \right\}} \right] \right]$$

(Eq. 2)

For a given voltage U, applied to the ESP, the ionic current I in eqs. 1 and 2 has to be found iteratively by numerical integration of the electric field, where the correct I fulfils the condition

$$U = - \int_{r_w}^r E dr \quad (\text{Eq. 3})$$

In combination with particle charging and deposition models, eqs. 1- 3 allow a stepwise calculation of the whole deposition process including the effect of particle space charge on ion and electric field distribution. Based on the assumption of fast lateral mixing and hence constant particle concentration and charge over the ESP's cross-section, an average gain in particle charge can be calculated from local charging kinetics. In combination with the deposition loss of charged particles that can easily be calculated from known particle electrical mobility and field strength at the surface of the collecting electrode, the rate of change in average particle charge, particle concentration and particle attached space charge concentration can be calculated. The result of this calculation method is compared to other model predictions in Fig. 2-5. However this calculation procedure is already quite complex.

2.2 Particle deposition in the strongly quenched regime

In case of very high particle concentration, the local current uptake level can be in the sub percent range of the clean gas current. Therefore, in the case of strong quenching, it is justified to neglect the contribution of the ionic space charge to the electric field.

In this case the drop of the electric potential over the particle attached space charge has to be equal to the difference between the applied voltage and the corona onset voltage. In this limiting case we find the electric field to be

$$E(r) = \frac{2\Delta U r}{r_i^2} + \frac{U_{onset}}{r \ln\left(\frac{r_i}{r_w}\right)}$$

(Eq. 4)

The space charge density which causes the drop of the electric potential between the corona wire and the tube is then found to be [1, 3]:

$$\rho_{i,p} = cne = \frac{4\epsilon_0 \Delta U}{r_i^2}$$

(Eq. 5)

Hence the particle number concentration c can be expressed by the average particle charge in the quenched regime.

$$c = \frac{4\epsilon_0 \Delta U}{ner_i^2}$$

(Eq. 6)

For a monodisperse aerosol one can derive a constant particle deposition rate based on the differential Deutsch-Anderson approach:

$$V \frac{dc}{dt} = -cAw_{sed} = cA \frac{neCu}{3\pi\eta x} E(r_i)$$

(Eq.7)

Solving this equation for dc/dt , writing $A/V=2/r$ for a tube, and substituting cne by eq. 5 and $E(r)$ from eq. 4, one finds a constant particle deposition rate in the strongly quenched regime [1, 3]:

$$\frac{dc}{dt} = -\frac{8\epsilon_0 \Delta U^2}{r_i^4} \frac{Cu}{3\pi\eta x} \left(2 + \frac{U_{onset}}{\Delta U \ln\left(\frac{r_i}{r_w}\right)} \right)$$

(Eq. 8)

Departing from the deposition rate and the initial aerosol concentration, we can derive a rough estimate of the residence time needed to overcome the quenched state (see Fig.2-5).

If additionally the limitation of the electric field by an excessive sparking frequency is considered, one can use eq. 8 for maximizing the deposition rate.

For example, a corona wire with 1mm diameter is chosen. The corresponding onset electric field is calculated by the Peek [5] formula. With the maximum average field U/r assumed to be 600 kV/m (typical value for dense sulphuric acid mist as given by Parker [4]) and the maximum electric field at the collecting electrode limited to 800kV/m, one finds tube diameter dependent deposition rates as shown in Fig.2-1 .

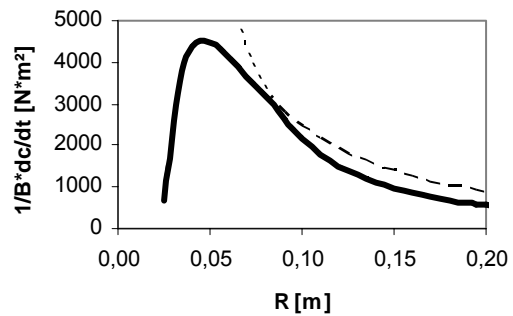


Fig. 2-1: Particle deposition rate divided by the particle electrical mobility as a function of the tube radius. Wire diameter: 1mm. Sparking criteria as described in text.

2.3 Particle concentrations which induce strong quenching

The continuous deposition of charged particles (eq. 8) while the particle attached space charge is assumed to be constant (eq. 5), implies that the particle charge must increase with time. Therefore a certain ion concentration and hence an ionic current must be present even in the strongly quenched regime.

For small currents, where the assumption of a negligible contribution of the ionic space charge is still justifiable, one can derive the time dependent current uptake from a balance of the particle attached space charge.

As the particle space charge concentration is assumed to constant in the quenched regime (eq. 5) it follows that the losses of particle space charge have to be compensated by an increase of average particle charge

$$\frac{d\rho_{i,p}}{dt} = ce \frac{dn}{dt} + ne \frac{dc}{dt} = 0$$

(Eq. 9)

And hence

$$c \frac{dn}{dt} = -n \frac{dc}{dt}$$

(Eq. 10)

whereby the particle deposition rate on the right hand side can be substituted by eq. 8.

The gain of the average particle charge can be calculated from an ion extinction function, if fast radial mixing and therefore constant particle concentration and average particle charge over the ESP's cross-section is assumed.

$$I(r_i) = I(r_w) \exp\left\{-c \int_n^{r_w} \frac{\Lambda}{Z_i E(r)} dr\right\}$$

(Eq. 11)

whereby the ion-particle combination coefficient Λ [m³/s] equals the particle charging rate in coulombs per second divided by the local ion space charge density. $\Lambda / (Z_i E)$ [m²] can be interpreted as the effective ion trapping cross section of a particle.

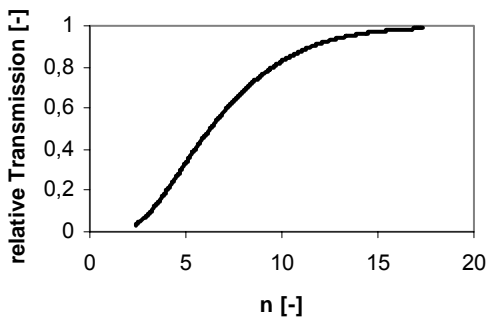


Fig. 2-2: Ion transmission through a 200nm aerosol ($\epsilon_r=2.1$) in ESP. Tube diameter: 0.2m, corona wire diameter 0.2mm, applied voltage 40kV. Λ according to Lawless [2] charging model.

The difference between the ionic current at the wire and at the precipitation electrode is the current which is attached to the particles and

leads to the increase of mean particle charge. So we find

$$c \frac{dn}{dt} = \frac{I(r_w)}{\pi r_i^2 L e} \left(1 - \exp\left\{ \frac{c}{Z_i} \int_{r_w}^{r_i} \frac{\Lambda}{E(r)} dr \right\} \right)$$

(Eq. 12)

Using eq. 12 for the left hand side of eq. 10 and the particle deposition rate in the quenched regime multiplied by the average particle charge for the right hand side, the ionic current uptake per meter of corona wire is the only unknown parameter. Substituting the concentration c by eq. 6, the solution of the resulting equation yields the specific current uptake:

$$\frac{I(r_w)}{L} = \frac{\frac{8 ne C U \epsilon_0}{3 \eta \pi r_i^2} \left(\Delta U U_{onset} \ln^{-1} \left(\frac{r_i}{r_w} \right) + 2 \Delta U^2 \right)}{1 - \exp\left\{ -\frac{4 \Delta U \epsilon_0}{n e r_i^2 Z_i} \int_{r_w}^{r_i} \frac{\Lambda}{E(r)} dr \right\}}$$

(Eq. 13)

Eq. 13 also allows to calculate the transmission of the ion current through the aerosol during the precipitation process. Fig. 2-2 shows the ion transmission as a function of average particle charge.

Of course, eq. 13 holds true only in the strongly quenched regime where ionic space charge is negligible. Therefore we define the strongly quenched regime to be restricted to current uptakes of less than five percent of the clean gas current. Fig. 2-3 shows the current uptake as a function of average particle charge as calculated by eq. 13 for Λ calculated by different charging theories.

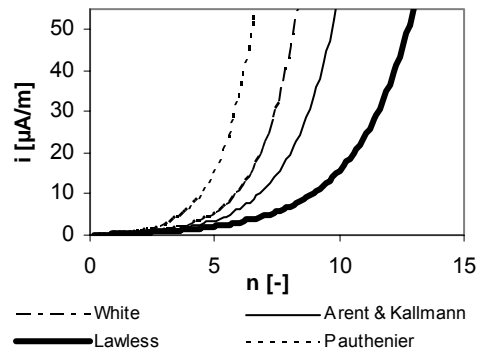


Fig. 2-3: Average charge dependent current uptake according to eq. 14 for different charging models. Aerosol and ESP as described in Fig. 2-2.

A correlation between average particle charge and residence time can be found from an

integration of the deposition kinetics, whereby the concentration $c(t)$ is substituted by eq. 6

$$i(n) = \frac{\frac{3\eta\pi x}{Cu} r_{tube}^4 \left(c_0 - \frac{4\epsilon_0 \Delta U}{ner_{tube}^2} \right)}{16\epsilon_0 \Delta U^2 \left(1 + \frac{U_{onset}}{2 \ln \left(\frac{r_{tube}}{r_{wire}} \right) \cdot \Delta U} \right)} \quad (\text{Eq. 14})$$

The combination of eq.13 and eq.14 allows the calculation of the residence time dependent specific current uptake as shown in Fig. 2-4. A comparison to other calculation methods is given in Fig. 2-5.

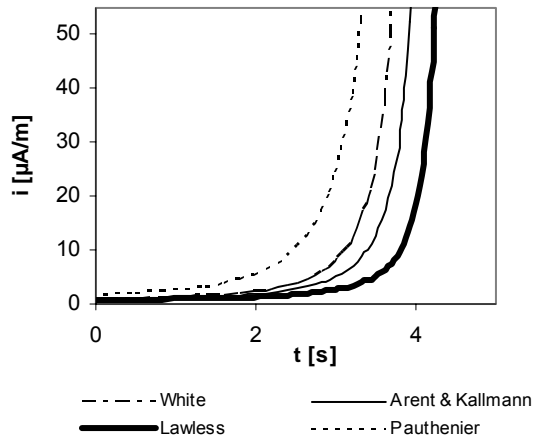


Fig. 2-4: Residence time dependent current uptake for data as used in Fig. 2-3 and an initial number concentration of $3 \cdot 10^{14} m^{-3}$. Clean gas current 1,1mA/m.

2.4 Simulations

Compared to the more or less analytical models presented above, numerical calculations additionally allow for the consideration of particle size distribution and distribution of particle charge within each size fraction.

Assuming negligible axial dispersion and radial symmetry of the system, the problem can be treated as 1-dimensional on the radius coordinate, while parameters are changing with time. The basic equations to be solved in a simulation are:

1) Equation of continuity for the ionic current, modified for ion losses due to particle charging.

$$\text{div}(\vec{i}) = \vec{i} \sum_{j=1}^{PC} \sum_{i=1}^{CC} c_{i,j} A_{ext,i,j} \quad (\text{Eq. 15})$$

whereby

$$A_{ext,i,j} = \frac{\Lambda_{j,k}(r)}{Z_i E(r)} \quad (\text{Eq. 16})$$

Here PC is the number of particle size classes and CC is the number of charge classes.

2) Poisson's equation

$$\text{div}(\vec{E}) = \frac{\rho_i + \rho_{i,p}}{\epsilon_0} \quad (\text{Eq. 17})$$

3) Electric potential

$$E = -\text{grad}(\varphi) \quad (\text{Eq. 18})$$

4) Particle charging kinetics

$$\left(\frac{dn}{dt} \right)_{j,k} = \frac{\rho_i}{e} \Lambda_{j,k} \quad (\text{Eq. 19})$$

5) Particle motion/-deposition (class-wise)

$$\vec{j}_{j,k} = c_{j,k} Z_{j,k} \vec{E} - D_{disp} \text{grad}(c_{j,k}) \quad (\text{Eq. 20})$$

For comparison of experimental and theoretical time dependent current uptake, the particle size distribution was discretized logarithmically into eight size fractions, the particle charge distribution within each size fraction was resolved down to one elementary charge and the radius was discretized linearly into 50 elements. A simulation for a monodisperse aerosol is show in Fig. 2-5 in comparison to the simpler models.

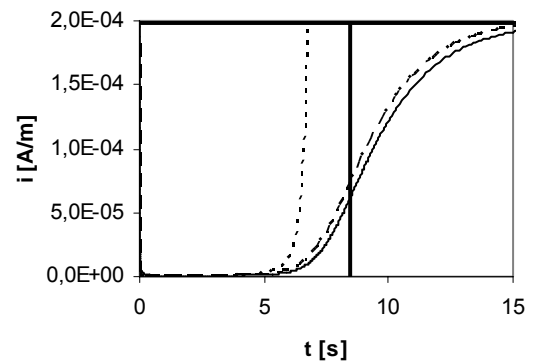


Fig. 2-5: Current uptake as a function of the residence time by a the assumption of a complete deposition under quenched conditions (fat solid line), by combination of eqs. 13 and 14 (short dashes), by the stepwise calculation using eqs. 1, 2 and 3 for calculation of ion and electric field distribution (long dashes), and by simulation (thin full line). Geometrical parameters of the ESP as in Fig. 2-2, applied voltage 20kV, particle diameter

200nm ($\epsilon_r=2.1$), initial number concentration 10^{14} m^{-3} .

Alltogether, these simulations are quite complex and probably, the analytical model prediction may be sufficient for design and trouble shooting in many cases.

2.5 Experimental validation of the model

A first series of experiments was carried out in an ESP that is operated in batch wise mode. This ESP consists of two tube wire type ESPs in parallel, which are connected on the top and bottom side. Each of these ESPs has a tube diameter of 0.2m and a wire diameter of 0.2mm. The total length of each ESP is 1.6m. To ensure well mixed conditions, fans were inserted into the connecting pieces between the two ESPs, which provide a circulating gas flow velocity of approximately 5m/s and maintain well mixed conditions.

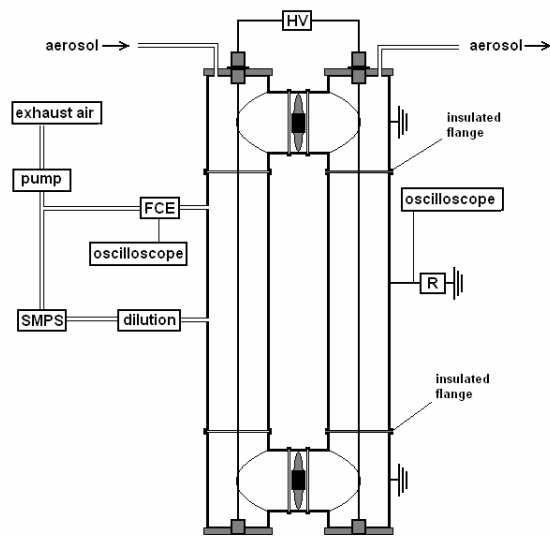


Fig. 2-6: Experimental setup for measurement of the time dependent current uptake.

The current uptake is measured from one of the two cylindrical sections by a digital recording oscilloscope via a 10 k Ω resistor. Sample points for the particle attached space charge density, measured by an FCE, and the particle size distribution and concentration by SMPS are located at the other tube.

As aerosol, a condensation aerosol of liquid paraffin was used.

For the positive corona the onset voltage was found to be 8.0 kV. The clean gas current voltage curve is in excellent agreement with

theoretical predictions [6] when the ion mobility is set to 1.55cm²/Vs.

The predicted space charge density in the quenched state (see eq. 2) is compared to measurement results in Fig. 2-7

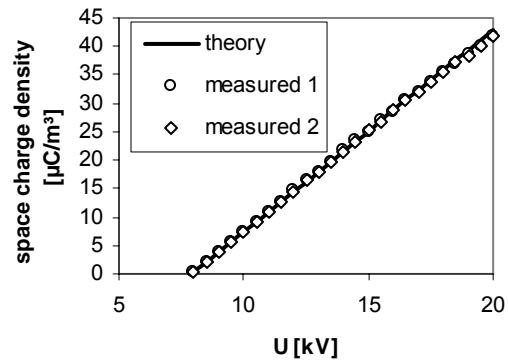


Fig. 2-7: Comparison of measured and predicted space charge density in the quenched regime.

For measurement of time dependent current uptake, the ESP was flushed with aerosol. Particle size distribution and concentration is measured by SMPS while flushing. When sampling was finished, the ESP was switched to the batch mode by closing the aerosol in and outlet. The voltage was switched on and the current was sampled as function of residence time. The current uptake characteristics for different applied voltages are compared to simulation predictions in Fig. 2-8.

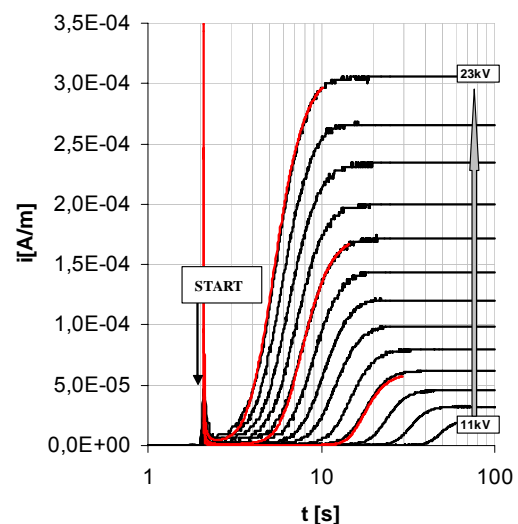


Fig. 2-8: Time dependent current uptake per length of corona wire for different applied voltages in comparison to simulations. Aerosol: liquid paraffin, $\epsilon_r=2.1$, $c_0 = 4.3 \cdot 10^{13} \text{ m}^{-3}$, CMD: 210nm, GSD: 1.4.

The residence times when the current approaches five percent of the clean gas current are

compared to the prediction of the analytical model in Fig. 2-9

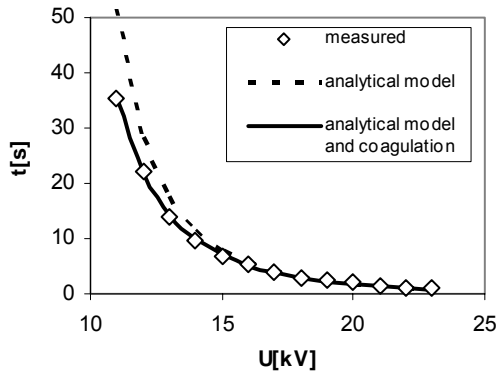


Fig. 2-9: Quenched residence time according to the current uptake measurements in Fig. 2-8 and prediction of the quench time by the analytical model with and without consideration of thermal coagulation. The CMD was used as particle size in the analytical model.

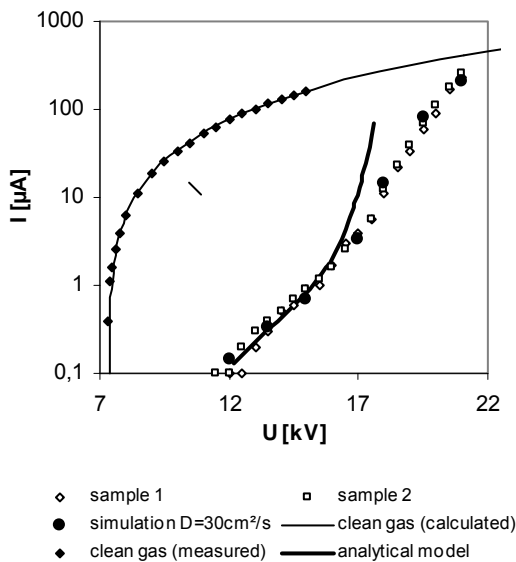


Fig. 2-10: Clean gas current voltage curve and current voltage curve under the influence of particle space charge for a continuously operated ESP.

To show the transferability of the findings to common continuously operated ESPs, the current voltage curve of a continuously operated ESP was measured under the influence of high particle concentration. The results are shown in Fig. 2-10 in comparison to the residence time averaged currents according to the analytical model and simulations.

3 Conclusion & Acknowledgement

Analytical models are able to describe current uptake and particle deposition quite well for strong corona quenching and allow to optimize dimensioning of wire-tube ESPs for quenched operation. With a 1D simulation, the transition from the quenched state to unquenched operation can be modelled with very good accuracy.

This project was supported by ELSTATIK Stiftung Guenter und Sylvia Luettgens, Odenthal, Germany, which is gratefully acknowledged.

4 Literature

- [1] Cooperman, P; Title: IEEE transactions on communication and electronics, vol. 48 (march 1963)
- [2] Lawless, P.A.: J. of Aerosol Science, 27, (1996) pp. 191-215
- [3] Matts, S., Lindau, L.: 2nd Int. Conf. on Electrostat. Prec., Kyoto (Nov. 1984), 911-919
- [4] Parker, K.: Applied Electrostatic Precipitation, Springer (1996)
- [5] Peek, F.W.: Dielectric Phenomena in High Voltage Engineering, McGraw-Hill (1929)
- [6] White, H.-J.: Industrial Electrostatic Precipitation Addison-Wesley Publ. Co (1963)

Symbols

A [m ²]:	collecting electrode area
A_{ext} [m ²]:	ion trapping cross section of a particle
B [m ² /(Ns)]:	mechanical particle mobility
Cu [-]:	Cunningham slip correction
c [1/m ³]:	number concentration
c_0 [1/m ³]:	initial number concentration
E [V/m]:	electric field strength
e [As]:	elementary charge
I [A]:	current
L [m]:	corona wire length
n [-]:	number of el. charges per particle
r [m]:	radius coordinate
r_t [m]:	tube radius
r_w [m]:	wire radius
t [s]:	residence time
U [V]:	voltage
ΔU :	difference betw. applied and onset voltage
V [m ³]:	precipitator volume
W_{sed} [m/s]:	particle drift velocity
x [m]:	particle diameter
Z_i [m ² /(Vs)]:	electrical mobility of the ions
ϵ_0 [As/(Vm)]:	electrical permittivity of vacuum
ρ_i [As/m ³]:	ion space charge density
$\rho_{i,p}$ [As/m ³]:	particle carried space charge density
Λ [m ³ /s]:	ion-particle combination coefficient
η [Pas]:	gas viscosity